ORIGINAL RESEARCH

H. Tanaka
N. Fujita
T. Enoki
K. Matsumoto
Y. Watanabe
K. Murase
H. Nakamura

Relationship between Variations in the Circle of Willis and Flow Rates in Internal Carotid and Basilar Arteries Determined by Means of Magnetic Resonance Imaging with Semiautomated Lumen Segmentation: Reference Data from 125 Healthy Volunteers

BACKGROUND AND PURPOSE: Volume flow rates in the feeding arteries of the brain are measured to evaluate blood flow dynamics in vascular disease. Although these flow values are thought to be effected by anatomic variations in the circle of Willis, few reports have described the effect. This study reports on the relationship between variations in the circle of Willis and volume flow rates in the bilateral internal carotid and basilar arteries of normal volunteers.

METHODS: We prospectively examined 125 healthy volunteers by MR imaging. Variations in the circle of Willis were classified as "textbook" type, hypoplasia of the precommunicating segment of the anterior cerebral artery (A1), hypoplasia of the precommunicating segment of the posterior cerebral artery (P1), or "other." Volume flow rates were measured by 2D cine phase-contrast MR imaging. Lumen boundaries and volume flow rates were semiautomatically determined by pulsatility-based segmentation.

RESULTS: Of the 117 subjects (61 men, 56 women; mean age, 23.6 years) considered suitable for flow measurement, 105 showed textbook type, and 6 each showed A1 hypoplasia and P1 hypoplasia. Total flow rates for the 3 variations were 781 ± 151 mL/min (mean ± SD), 744 ± 119, and 763 ± 129, respectively. Relative contributions by flow rates of the internal carotid arteries and the basilar artery for the 3 variations were 39.8%:38.9%:21.3%, 31.8%:49.1%:19.0%, and 46.6%:41.6%:11.7%, respectively, showing statistically significant differences.

CONCLUSIONS: Variations in the circle of Willis correlate significantly with relative contributions by the flow rates of the bilateral internal carotid and basilar arteries.

Volume flow rates in the feeding arteries of the brain, such as the internal carotid artery and the basilar artery, have been used to evaluate blood flow dynamics in vascular disease.[1-4] For these evaluations, reference data of volume flow rates in normal subjects are essential and have been reported by several investigators.[5,6] In these studies, however, anatomic variations in the circle of Willis that presumably effect the volume flow rates in the feeding arteries have not been mentioned.[5,6] Nevertheless, variations in the circle of Willis are common. For instance, the hypoplastic precommunicating segment of the anterior cerebral artery (A1) is found in 1%–16% of subjects,[7-10] and the hypoplastic precommunicating segment of the posterior cerebral artery (P1) is found in 4%–14% of subjects.[7,8] Accordingly it is important to obtain reference data of volume flow rate for these common variations. Correlation between anatomic variation in the circle of Willis and volume flow rates in the internal carotid arteries and the basilar artery has been investigated.[11] Although its findings were significant, the subjects were patients with symptomatic atherosclerosis or risk factors for atherosclerosis.[11] We believe, therefore, that it is still important to establish other reference data, obtained from healthy subjects, that, to the best of our knowledge, have not been reported.

The purpose of this study was thus to determine the relationship between variations in the circle of Willis and volume flow rates in the bilateral internal carotid arteries and the basilar artery in healthy volunteers.

Materials and Methods

Subjects

This prospective study was approved by our institutional review board. The subjects were 125 healthy volunteers (63 men, 62 women) who had given their written informed consent. Inclusion criteria were: (1) age between 20 and 29 years, (2) no past history of or present neurologic disorders, (3) no past history of or present cardiovascular disorders, (4) no contraindications, such as claustrophobia or pregnancy, for MR examination, and (5) no use of medication.

MR Studies

All MR studies were performed on a 1.5T imager with a commercially available head coil. The subject was supine with the neck and head in the neutral position. MR examination consisted of 3D time-of-flight MR angiography, 2D cine phase-contrast MR imaging, and fast spin-echo T2-weighted axial imaging (repetition time [TR]/effective echo time [TE$_{eff}$], 4000/101 ms; matrix, 256 × 256; field of view [FOV], 200 mm; section thickness, 5 mm). The purpose of the T2-weighted
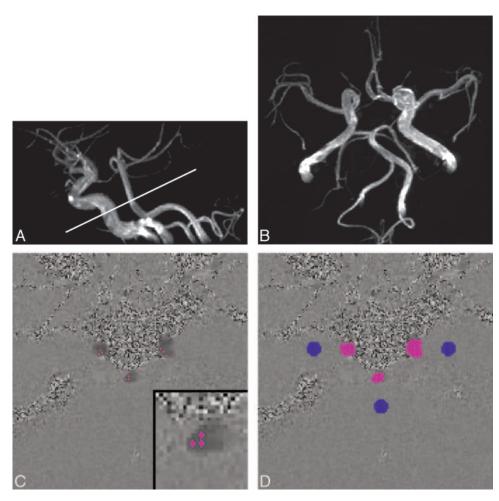
Fig 1. MR examination and flow measurement procedures for a representative case (23-year-old woman).

A, Lateral view of 3D time-of-flight MR angiography. The white line indicates the section used for the phase-contrast MR imaging.

B, Axial view of 3D time-of-flight MR angiography. The variation in the circle of Willis in this case was assessed as hypoplasia of the precommunicating segment of the right anterior cerebral artery (right A1 hypoplasia) based on diameter measurements obtained from the original MR angiography images.

C, As the first step of flow measurement, an operator selected 3 pixels from each artery. These pixels are shown as red dots in this phase-contrast image. The *inset* in the *bottom right corner* shows a magnified image of the basilar artery for instance.

D, From these selected pixels, vessel lumens (*clusters of red dots*) were automatically identified by pulsatility-based segmentation.[17] To compensate for eddy current-induced error, 3 static regions of interest (*clusters of blue dots*) were also determined automatically. This compensation was based on the assumption that the error induced by the eddy current was a linear function of space.[14] Eventually volume flow rate of each artery was automatically obtained.

images was to make sure that there were no abnormalities or lesions in the brain.

Variations in the circle of Willis were classified using 3D time-of-flight MR angiography (TR/echo time [TE], 35/4.7 ms; flip angle, 20°; matrix, 256 × 256; FOV, 200 mm; slab thickness, 52.8 mm; section thickness, 0.8 mm) combined with the magnetization transfer technique. In addition, zero-interpolation was applied to the frequency, phase, and section selection axes to reduce the pixel width by half. Another purpose of this scan was to measure the angle between the scanning plane of the 2D cine phase-contrast image and the arteries. The measurement error of 2D cine phase-contrast MR imaging is smallest when the scanning plane is perpendicular to a vessel. Because we wanted to measure the volume flow rates of 3 vessels using a single section, it was inevitable that the plane be set at an angle less than perpendicular to the vessel. Deviation from the perpendicular of the angle between the scanning plane and the vessel results in overestimation of the volume flow rate.[12,13] A previous study, using vessel diameter/section thickness and vessel diameter/resolution ratios similar to those used in our study, demonstrated that the error is less than 15% when the deviation of the angle is less than 30°.[13] With these considerations in mind, we measured the angle between the scanning plane of the 2D cine phase-contrast image and the arteries immediately after setting the scanning plane. If the angle was more than 30° from the perpendicular, a new scanning plane of the phase-contrast image was used.

Volume flow rates in the bilateral carotid arteries and the basilar artery were measured by 2D cine phase-contrast MR imaging with retrospective gating, which can detect velocity in the section select direction.[14] The previously obtained MR angiograms were used to plan the phase-contrast MR imaging at the skull base as perpendicularly as possible to internal carotid arteries and the basilar artery[5] (Fig 1A). For the internal carotid arteries, measurements were performed at a relatively straight section consisting of the posterior ascending portion of the cavernous segment and the distal portion of the lacerum segment. For the basilar artery, volume flow rates were measured at the middle portion, which lies between the origin of the anterior inferior cerebellar arteries and that of the superior cerebellar arteries.

Other parameters of 2D cine phase-contrast imaging were as follows (TR/TE, 24/6.6–7.2 ms; flip angle, 30°; matrix, 256 × 256; FOV, 120 mm; section thickness, 5 mm, number of cardiac phases, 16). The flip angle, FOV, and matrix were decided based on the findings of previous studies.[12,13,15] Encoding velocity was set at 100 cm/s. If aliasing was noted, the imaging was repeated with an encoding velocity of 150 cm/s.

Overall Inspection of MR Images
Before further analysis, MR images were examined by a radiologist for the detection of lesions or image degradation, and if either was found to render the data unsuitable for the further analysis, the subject was excluded.

Classification of Variations in the Circle of Willis
After inspection, the 3D time-of-flight MR angiography images were transferred to a workstation. The diameters of bilateral A1 and P1
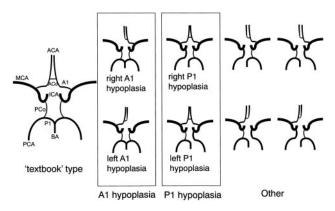
Fig 2. Classification of the anatomic variations in the circle of Willis. In the "textbook" type, both the precommunicating segment of the anterior cerebral artery (A1) and that of the posterior cerebral artery (P1) were normal in size. The next group included both right and left A1 hypoplasia. Because no significant difference between cerebral arteries on the right and left sides has been established,[5,18] we combined right and left A1 hypoplasia into A1 hypoplasia. The next group included right and left P1 hypoplasia, which again were treated as a single category, P1 hypoplasia. "Other" type included a combination of A1 hypoplasia and P1 hypoplasia, bilateral P1 hypoplasia, as well as other unclassified variations. ACA indicates anterior cerebral artery; ACo, anterior communicating artery; MCA, middle cerebral artery; ICA, internal cerebral artery; PCo, posterior communicating artery; PCA, posterior cerebral artery; BA, basilar artery

were measured on the original 3D time-of-flight MR angiography images.

Threshold of hypoplasia was set at 1.0 mm for our study; in other words, if the diameter was less than 1.0 mm, the artery was judged to be hypoplastic. This threshold, which was 2.5 times larger than our resolution after zero interpolation, was used in autopsy studies[9,10] and an MR study.[16] Because we were interested in the relative contribution by the bilateral carotid and the basilar arteries, hypoplasia of A1 and of P1 were important for the classification, whereas the size of the anterior communicating artery, for example, was irrelevant as long as bilateral A1 was normal in size. On this basis, variations in the circle of Willis were classified as seen in Fig 2. Among these variations, we measured the volume flow rate only for "textbook" type, A1 hypoplasia, and P1 hypoplasia variations.

Volume Flow Rate Measurement

In a separate approach, the 2D cine phase-contrast images were examined by another investigator who was blind to the subject's variation in the circle of Willis.

For definition of the lumen, we used pulsatility-based segmentation.[17] Because velocity was measured at 16 phases of the cardiac cycle with the cine phase-contrast technique, the waveform representing velocity versus cardiac phase was obtained for each pixel. After a pixel obviously inside the lumen was selected, the correlation coefficient could be calculated for the velocity versus cardiac phase waveform of the pixel and the waveform of the other pixels in the images. The threshold value of the correlation coefficient, which determines the vessel boundary, depends on specific flow type and scanning parameters and lies somewhere around 0.5 and 0.7.[17] We adopted 0.6 as the optimal threshold based on the preliminary results for 7 volunteers using the same parameters as those used for the study presented here. Therefore, the vessel lumen was defined as a cluster of pixels showing a correlation coefficient greater than or equal to 0.6[17] (Fig 1, *C* and *D*).

During this procedure, the only responsibility of the operator was to identify reference pixels inside the lumen. Although it is difficult to manually determine the lumen boundary, it is relatively easy to iden-

tify reference pixels in the lumen, meaning that this semiautomated method is minimally dependent on the operator.

Statistical Analysis

Previous studies[5,6] have reported that the cerebral blood flow rate varies considerably among subjects. For example, the maximum cerebral blood flow is approximately twice as great as the minimum cerebral blood flow for the same age range.[5,6] For this reason, differences of flow rate due to variations in the circle of Willis can be blurred by these large intersubject variations. Because relative percentage contributions are presumably less affected by intersubject variations, we compared relative percentage contributions, rather than absolute values to determine the relationship between variations in the circle of Willis and flow rates of each artery.

We used one-factor analysis of variance (ANOVA) with variation in the circle of Willis as the factor for this comparison. When a variation showed a statistically significant effect, the Tukey-Kramer post hoc test was used. Overall risk for type 1 errors was set at 5%. Because the ANOVA and subsequent post hoc test were performed 3 times, statistical significance was set at 1% for each ANOVA and post hoc test.

Results

Of the 125 subjects who underwent MR examination, 6 were excluded at "overall inspection of MR images" because of the following reasons for 1 of each of these subjects. A 3-mm sized lesion with high signal intensity on T2-weighted image was detected. It was impossible to perform phase-contrast imaging without violating angle criteria. Aliasing was noted in phase-contrast images with encoding velocity of 100 cm/s and those with 150 cm/s were not obtained. Scan location of the phase-contrast image was too caudal. The image was degraded due to metal in the mouth. There was a left persistent trigeminal artery. Two more subjects were excluded at "volume flow rate measurement," because the vessel lumen could not be identified by pulsatility-based segmentation. Both subjects had the "textbook" type of the circle of Willis.

The results reported here are thus of the remaining 117 subjects comprising 56 women and 61 men with an age from 20 to 29 years (23.6 ± 2.9; mean ± SD). "Textbook" type was observed in 105, and A1 and P1 hypoplasia variations in 6 subjects each. For these 6 subjects with A1 hypoplasia and 6 with P1 hypoplasia, Table 1 shows diameters of the bilateral A1 and P1, volume flow rates, and their relative percentage contribution.

Variations in the Circle of Willis Versus Volume Flow Rate

Total volume flow rate and volume flow rates of each artery are shown in Table 2. Relative contributions of the arteries for the 3 variations in the circle of Willis are summarized in Fig 3. One-factor ANOVA showed an overall effect by the variation in the circle of Willis (*P* < .0001) in each artery. The Tukey-Kramer post hoc test, using 0.01 as statistical significance threshold, was then performed for each artery and disclosed the following significant differences. The relative contributions of the internal carotid arteries ipsilateral and contralateral to hypoplastic A1 are significantly smaller and significantly larger than that of the internal carotid artery in the "textbook" type, respectively. The relative contribution of the

Table 1: Diameters of A1 and P1 and volume flow rates of 6 subjects with A1 hypolasia (nos. 1–6) and 6 with P1 hypoplasia (nos. 7–12)

| | Diameter (mm) | | | | Volume Flow Rates (mL/min) (Relative Percentage Contribution (%)) | | |
| | Ipsilateral to Hypolastic A1 or P1 | | Contralateral to Hypoplastic A1 or P1 | | ICA Ipsilateral to Hypoplastic A1 or P1 | ICA Contralateral to Hypoplastic A1 or P1 | Basilar Artery |
Subject No.	A1	P1	A1	P1			
1	0.0*	2.3	1.4 + 1.3†	2.4	267 (29)	468 (51)	188 (20)
2	0.7	1.0	2.0	1.7	305 (38)	405 (51)	88 (11)
3	0.9	2.0	2.7	2.4	257 (32)	380 (47)	166 (21)
4	0.8	1.4	1.5	2.1	212 (35)	274 (45)	119 (20)
5	0.0*	1.8	2.3	2.0	179 (26)	348 (50)	169 (24)
6	0.0*	1.9	2.7	2.0	199 (31)	325 (51)	116 (18)
7	1.5	0.8	2.2	2.1	438 (48)	349 (38)	120 (13)
8	1.8	0.9	2.2	1.4	298 (44)	303 (45)	76 (11)
9	1.3	0.9	1.7	2.0	379 (52)	254 (35)	91 (13)
10	2.1	0.8	2.0	1.1	296 (48)	266 (43)	52 (8)
11	1.4	0.0*	2.0	1.8	300 (42)	312 (43)	108 (15)
12	1.5	0.9	2.5	1.9	422 (45)	418 (45)	95 (10)

Note:—A1 indicates precommunicating segment of the anterior cerebral artery; P1, precommunicating segment of the posterior cerebral artery; ICA, internal carotid artery. An artery with a diameter ≤0.9 mm was considered to be hypoplastic.
* The relevant artery was not depicted.
† Duplicate A1s were observed.

Table 2: Variations in the circle of Willis and volume flow rates

Variations in the Circle of Willis	"Textbook" Type (*n* = 105)	A1 Hypoplasia (*n* = 6)	P1 Hypoplasia (*n* = 6)
Total volume flow (mL/min) (mean ± SD)	781 ± 151	744 ± 119	763 ± 129
Right internal carotid artery or internal carotid artery ipsilateral to hypoplastic A1 or P1	311 ± 73	236 ± 48	355 ± 66
Left internal carotid artery or internal carotid artery contralateral to hypoplastic A1 to P1	304 ± 74	367 ± 67	317 ± 60
Basilar artery	165 ± 43	141 ± 39	90 ± 24

Note:—A1 indicates precommunicating segment of the anterior cerebral artery; P1, precommunicating segment of the posterior cerebral artery.

internal carotid artery ipsilateral to hypoplastic P1 is significantly larger and that of the basilar artery in P1 hypoplasia variation is significantly smaller than that of the corresponding artery in the "textbook" type.

Discussion

Correlation between Anatomic Variations in the Circle of Willis and Volume Flow Rates of the Proximal Arteries
Volume flow rates in the feeding arteries of the brain have been used to evaluate blood flow dynamics in patients with vascular disease. However, asymmetries of flow rates or low flow rates in specific arteries found in these patients do not necessarily mean the presence of vascular disease; they may be due to variations in the circle of Willis.

In this study, we measured volume flow rates of the bilateral internal carotid arteries and the basilar artery in 125 healthy volunteers and found that the relative contribution of each of the proximal arteries correlates significantly with variations in the circle of Willis. We also obtained relative flow contributions by the proximal arteries for common variations of the circle of Willis, which can be used as reference data.

Hendrikse et al[11] recently investigated the same item as that examined in our study in patients with symptomatic atherosclerosis or risk factors for atherosclerosis but without significant (>70%) stenosis. Absence or presence of brain lesions such as an infarction was not detailed in their report. Although their results were the same as ours, there are several differences

between our study and that by Hendrikse et al,[11] such as subjects (healthy volunteers instead of patients), MR phase-contrast technique (cine and ungated), classification of the variation in the posterior part of the circle of Willis (P1 hypoplasia rather than fetal-type posterior cerebral artery), and lumen segmentation (semiautomated and manual drawing).[11] Moreover, pulsatility-based semiautomatic segmentation as used in our study is reportedly more accurate and more reproducible than manual drawing.[17] We therefore believe our methods are more appropriate for obtaining reference data.

Effect of Vessel Size on Measurement Error with Pulsatility-Based Segmentation
Pulsatility-based segmentation was used to segment vessel lumen in this study. The original article describing this segmentation method mentions that a phantom study using 8- and 5-mm diameter tubes was performed.[17] This method yielded accurate results for the 8-mm tube but overestimated results for the 5-mm tube, though the error of the volume flow rate was smaller than that by manual drawing.[17] According to the discussion in this article,[17] the overestimation was due in part to the partial volume effect, because boundary pixels that occupy both stationary and flowing spins are likely to be included into the lumen by pulsatility-based segmentation. Because the ratio of the number of boundary pixels to the total number of pixels of the lumen is larger for smaller vessels, overestimation of size can be expected to increase for smaller vessels.
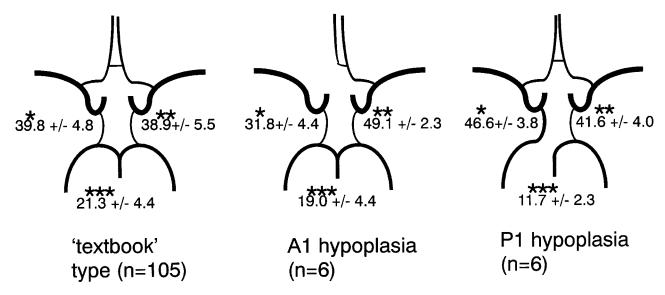
Fig 3. Relative contribution of proximal arteries to total volume flow in variations in the circle of Willis. Values signify mean percentage ± SD. The *upper left* value corresponds to the relative contribution of the right internal carotid artery in the "textbook" type or of the internal carotid artery ipsilateral to hypoplastic A1 or P1 in the other variations. The *upper right* value corresponds to the relative contribution of the left internal carotid artery in the "textbook" type, or of the internal carotid artery contralateral to hypoplastic A1 or P1 in the other variations. The value at the bottom corresponds to the relative contribution of the basilar artery.

* The value for A1 hypoplasia variation was significantly smaller than those for "textbook" type and P1 hypoplasia variation. The value for P1 hypoplasia variation was significantly larger than that for "textbook" type.

** The value for A1 hypoplasia variation was significantly larger than that for "textbook" type.

*** The value for P1 hypoplasia variation was significantly smaller than that for "textbook" type.
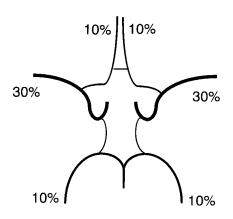

Fig 4. Estimated volume flow ratio of the anterior, middle, and posterior cerebral artery. These values were estimated from Fig 3 and approximated to multiples of 10%.

The respective diameters of the internal carotid and basilar arteries where we measured the volume flow rate were approximately 4.5 and 3 mm. Because the pixel size was not mentioned in the article,[17] we cannot estimate the errors of measurement for our vessels based on those for the phantom tubes reported in the article.[17] Instead, we estimated errors of measurement as follows. With our pixel size of 0.5 mm, the number of the boundary pixels is approximately 23, and those included completely in the lumen is approximately 18 for a 3-mm diameter vessel. If the boundary pixels are segmented as the lumen, the vessel size will be overestimated by 20%. Because the velocity of flowing blood is slower at boundary than at the midportion of the lumen and because phase change in the boundary pixels is reduced with static spins, overestimation of the volume flow rate is probably less than 20%. For instance, overestimation of size was 14%, whereas overestimation of the volume flow rate was

4.5% for the 5-mm diameter phantom used in the article of pulsatility-based segmentation.[17]

Estimated Distribution of Flow to Efferent Arteries

Distribution of flow to efferent arteries of the circle of Willis, such as the anterior, middle, and posterior cerebral arteries, can be estimated and approximated to multiples of 10%. If we round the values in Fig 3 to multiples of 10%, the respective ratios of contribution to the bilateral internal carotid arteries and the basilar artery would be 40:40:20, 30:50:20, and 50:40:10 for the "textbook" type, A1 hypoplasia variation, and P1 hypoplasia variation, respectively. Assuming that both anterior cerebral arteries are supplied by a single internal carotid artery in the A1 hypoplasia variation and that the posterior cerebral artery ipsilateral to hypoplastic P1 is supplied only by the posterior communicating artery in the P1 hypoplasia variation, the relative flow rates of the anterior, middle, and posterior cerebral arteries would be 10%, 30%, and 10%, respectively (Fig 4).

Few studies have dealt with the flow distribution of efferent arteries. Enzmann et al[18] used cine phase-contrast MR imaging to measure the blood volume flow in 10 healthy volunteers. They directly measured volume flow rates of the anterior cerebral artery, middle cerebral artery, posterior cerebral artery, internal carotid artery, and basilar artery and reported relative flow rates of the anterior, middle, and posterior cerebral arteries to be 34:46:20,[18] which is different from our estimate. The sum of the reported values of the bilateral internal carotid arteries and the basilar artery was 800 mL/min, whereas that of the bilateral anterior, middle, and posterior cerebral arteries was 502 mL/min.[18] We think a difference of 298 mL/min is too large for branches, such as the ophthalmic artery and superior cerebellar artery. Because flow rates of the

internal carotid and the basilar arteries reported in this study[18] were similar to those obtained by other studies with MR imaging[5] and sonography,[6] the difference may be caused by the difficulty of accurately measuring the volume flow in small vessels such as the anterior cerebral artery. In addition, Gobin et al estimated the vascular territory to decide dose of intra-arterial chemotherapy for brain tumors.[19] They estimated "on the basis of their experience with selective catheterization and anatomic knowledge of the vascular territories of the major brain arteries." Their ratio for anterior cerebral artery/middle cerebral artery/posterior cerebral artery was 1:3:0.75, which is similar to our estimate.

Limitations of this Study

There are several limitations to our study, one of which is that the lumen of 2 subjects could not be identified. This was presumably because the pulsation was insufficient to identify the lumen with the correlation coefficient method. However, the incidence of this occurrence was only 2 of 119 or <2%. We therefore do not think this limitation seriously biased our results.

Another limitation is that vessels with a slow flow may not show a high signal intensity on time-of-flight MR angiography due to saturation effect, in which case even a large artery cannot be visualized and may be erroneously classified as a hypoplastic artery. However, because an artery with a slow flow is equivalent to a hypoplastic artery in terms of flow rate, this limitation is probably unimportant for our study.

In conclusion, variations in the circle of Willis significantly correlate with the relative contributions of the flow rates of proximal arteries and should therefore be taken into consideration when interpreting results of flow rate measurements.

References

1. Rutgers DR, Klijn CJM, Kappelle LJ, et al. **Recurrent stroke in patients with symptomatic carotid artery occlusion is associated with high-volume flow to the brain and increased collateral circulation.** *Stroke* 2004;35:1345–49
2. Van den Boom R, Lesnik Oberstein SA, Spilt A, et al. **Cerebral hemodynamics and white matter hyperintensities in CADASIL.** *J Cereb Blood Flow Metab* 2003;23:599–604
3. Kato T, Indo T, Yoshida E, et al. **Contrast-enhanced 2D cine phase MR angiography for measurement of basilar artery blood flow in posterior circulation ischemia.** *AJNR Am J Neuroradiol* 2002;23:1346–51
4. Rutgers DR, Blankensteijn JD, Van der Grond J. **Preoperative MRA flow quantification in CEA patients: flow differences between patients who develop cerebral ischemia and patients who do not develop cerebral ischemia during cross-clamping of the carotid artery.** *Stroke* 2000;31:3021–28
5. Buijs PC, Krabbe-Hartkamp MJ, Bakker CJG, et al. **Effect of age on cerebral blood flow: measurement with ungated two-dimensional phase-contrast MR angiography in 250 adults.** *Radiology* 1998;209:667–74
6. Scheel P, Ruge C, Petruch UR, et al. **Color duplex measurement of cerebral blood flow volume in healthy adults.** *Stroke* 2003;31:147–50
7. Krabbe-Hartkamp MJ, Van der Grond J, De Leeuw FE, et al. **Circle of Willis: morphologic variation on three-dimensional time-of-flight MR angiograms.** *Radiology* 1998;207:103–11
8. Puchades-Orts A, Nombela-Gomez M, Ortuño-Pacheco G. **Variation in form of circle of Willis: some anatomical and embryological considerations.** *Anat Rec* 1976;185:119–23
9. Battacharji SK, Hutchinson EC, McCall AJ. **The circle of Willis—the incidence of developmental abnormalities in normal and infarcted brains.** *Brain* 1967;90:747–58
10. Alpers BJ, Berry RG, Paddison RM. **Anatomical studies of the circle of Willis in normal brain.** *Arch Neurol Psychiatr* 1959;81:409–18
11. Hendrikse J, Van Raamt AF, Van der Graaf Y, et al. **Distribution of cerebral blood flow in the circle of Willis.** *Radiology* 2005;235:184–89
12. Tang C, Blatter DD, Parker DL. **Accuracy of phase-contrast flow measurements in the presence of partial-volume effects.** *J Magn Reson Imaging* 1993;3:377–85
13. Wolf RL, Ehman RL, Riederer SJ, et al. **Analysis of systematic and random error in MR volumetric flow measurements.** *Magn Reson Med* 1993;30:82–91
14. Pelc NJ, Sommer FG, Li KCP, et al. **Quantitative magnetic resonance flow imaging.** *Magn Reson Q* 1994;10:125–47
15. Bakker CJG, Hoogeveen RM, Viergever MA. **Construction of a protocol for measuring blood flow by two-dimensional phase-contrast MRA.** *J Magn Reson Imaging* 1999;9:119–27
16. Schomer DF, Marks MP, Steinberg GK, et al. **The anatomy of the posterior communicating artery as a risk factor for ischemic cerebral infarction.** *N Engl J Med* 1994;330:1565–70
17. Alperin N, Lee SH. **PUBS: Pulsatility-based segmentation of lumens conducting non-steady flow.** *Magn Reson Med* 2003;49:934–44
18. Enzmann DR, Ross MR, Marks MP, et al. **Blood flow in major cerebral arteries measured by phase-contrast cine MR.** *AJNR Am J Neuroradiol* 1994;15:123–29
19. Gobin YP, Cloughesy TF, Chow KL, et al. **Intraarterial chemotherapy for brain tumors by using a spatial dose fractionation algorithm and pulsatile delivery.** *Radiology* 2001;218:724–32